Expression Patterns of a twist-Related Gene in Embryos of the Spider Achaearanea tepidariorum Reveal Divergent Aspects of Mesoderm Development in the Fly and Spider

Authors: Yamazaki, Kazunori, Akiyama-Oda, Yasuko, and Oda, Hiroki

Source: Zoological Science, 22(2) : 177-185

Published By: Zoological Society of Japan

URL: https://doi.org/10.2108/zsj.22.177

ZOOLOGICAL SCIENCE **22**: 177–185 (2005)

Expression Patterns of a *twist*-Related Gene in Embryos of the Spider *Achaearanea tepidariorum* Reveal Divergent Aspects of Mesoderm Development in the Fly and Spider

Kazunori Yamazaki[1†], Yasuko Akiyama-Oda[1,2] and Hiroki Oda[1*]

[1]*JT Biohistory Research Hall, 1-1 Murasaki-cho, Takatsuki, Osaka 569-1125, Japan*
[2]*PRESTO, Japan Science and Technology Agency*

ABSTRACT—We cloned an *Achaearanea tepidariorum* (Chelicerata, Arachnida) gene related to *Drosophila twist (twi)*, which encodes a basic helix-loop-helix transcription factor required to specify mesoderm fate in the *Drosophila* embryo. The cloned spider gene was designated *At.twist* (*At.twi*). We examined its expression by whole-mount in situ hybridization. *At.twi* transcripts were first detected in cells located at the polar and equatorial areas of the spherical embryo when the cumulus reached the equator. As the extra-embryonic area expanded, more cells expressed *At.twi* transcripts. The *At.twi*-expressing cells became distributed nearly uniformly in the embryonic area. At these stages, some *At.twi*-expressing cells were found in the surface epithelial cell layer, but other *At.twi*-expressing cells were at slightly deeper positions from the surface. When the embryo was transformed into a germ band, all *At.twi*-expressing cells were situated just beneath the surface ectoderm, where they became metamerically arranged. Although little expression was observed in the caudal lobe of the elongating germ band, new stripes of *At.twi* expression appeared beneath the ectoderm in accordance with the posterior growth. These observations suggested that the cells expressing *At.twi* were most likely mesoderm. We propose that *At.twi* can be used as a molecular marker for analyzing mesoderm development in the spider embryo. Moreover, comparison of the expression patterns of *twi* and *At.twi* revealed divergent aspects of mesoderm development in the fly and spider. In addition, we cloned an *Achaearanea* gene related to *snail,* which is another *mesoderm-determining* gene in *Drosophila,* and showed that its expression was restricted to the ectoderm with no indication for a role in mesoderm development.

Key words: chelicerate, arthropod, mesoderm development, *twist, snail*

INTRODUCTION

The mesoderm is the third germ layer that emerges between the ectoderm and endoderm during the development of bilaterians. Since the mode of mesoderm development among bilaterian taxa varies markedly, it seems almost impossible to reconstruct the evolution of mesoderm development based solely on morphological data.

In *Drosophila*, the molecular mechanisms that specify the fate of the primary mesoderm and regulate the development of the mesoderm have been extensively studied. In the syncytial blastoderm, maternal gene products establish morphogen gradients that define the anterior-posterior (AP) and dorsal-ventral (DV) axes (St Johnston and Nüsslein-Volhard, 1992). The nuclear gradient of Dorsal protein along the DV axis directly regulates the transcription of zygotic genes in a concentration-dependent manner, resulting in region-specific gene expression (Chasan and Anderson, 1993). At the ventral one-fourth region of the blastoderm, transcription of *twist (twi)* and *snail (sna)* is activated, which are essential for mesoderm formation (Simpson, 1983; Leptin and Grunewald, 1990). The *twi* gene, encoding a basic helix-loop-helix (bHLH) transcription factor (Thisse and Thisse, 1992), activates the transcription of mesoderm-specific genes (Leptin, 1991; Furlong *et al*., 2001). The *sna* gene, encoding a zinc-finger transcription factor (Boulay *et al*., 1987), mainly represses the transcription of ectodermal genes (Leptin, 1991). Such positive and negative regulation by *twi* and *sna* specifies the primary mesoderm at the ventral region. The *twi* gene continues to be expressed in all cells of the mesoderm until they extend over the whole of the inner surface of the ectoderm (Thisse *et al*., 1988). During the patterning of the mesoderm, *twist* expression is reg-

* Corresponding author. Phone: +81-726-81-9751;
Fax : +81-726-81-9757;
E-mail: hoda@brh.co.jp
† Present address: Department of Biological Sciences, Graduate School of Science, University of Tokyo, Tokyo 113-0033, Japan

ulated by *wingless*, *hedgehog*, and *Notch* signaling (Lee and Frasch, 2000; Riechmann *et al.*, 1997; Tapanes-Castillo and Baylies, 2004). *sna* expression disappears from the mesoderm soon after the internalization (Alberga *et al.*, 1991). Signals from the surface ectoderm also contribute to mesoderm development (Staehling-Hampton *et al.*, 1994).

Characterization of the *dorsal*, *twi* and *sna* homologs in another insect, *Tribolium*, revealed a conserved mechanism of mesoderm formation in long- and short-germ insects (Sommer and Tautz, 1994; Chen *et al.*, 2000). Even in non-arthropod metazoans, *twi* homologs have been identified and shown to be expressed in mesoderm- or endoderm-derived tissues (Hopwood *et al.*, 1989; Yasui *et al.*, 1998; Harfe *et al.*, 1998; Imai *et al.*, 2003; Nederbragt *et al.*, 2002; Spring *et al.*, 2000; Martindale *et al.*, 2004). However, none of these non-arthropod *twist* genes appear to function in the specification of the primary mesoderm. Moreover, in non-insect arthropods, few molecular data concerning mesoderm development are available.

To investigate the variation in the mode of mesoderm development among arthropods, we employed embryos of the spider *Achaearanea tepidariorum*. This animal belongs to Chelicerata, which is phylogenetically distant from Insecta within Arthropoda (Friedrich and Tautz, 1995; Boore *et al.*, 1998; Giribet *et al.*, 2001; Cook *et al.*, 2001). Although many previous works have described the embryonic development of spiders and other chelicerates (Montgomery, 1909; Holm, 1940, 1952; Seitz, 1966; Anderson, 1973; Yoshikura, 1975; Suzuki and Kondo, 1995), it is largely unclear how the mesoderm is formed and patterned during chelicerate development due to technical limitations in identifying mesoderm cells. The stages of *Achaearanea* embryogenesis that have been defined on the basis of morphological characteristics in living embryos (Akiyama-Oda and Oda, 2003) are illustrated in Fig. 1. In the *Achaearanea* embryo, several morphologically distinct cell types have been observed beneath the surface ectoderm at the cumulus-migrating and later stages (Montgomery 1909; Akiyama-Oda and Oda, 2003).

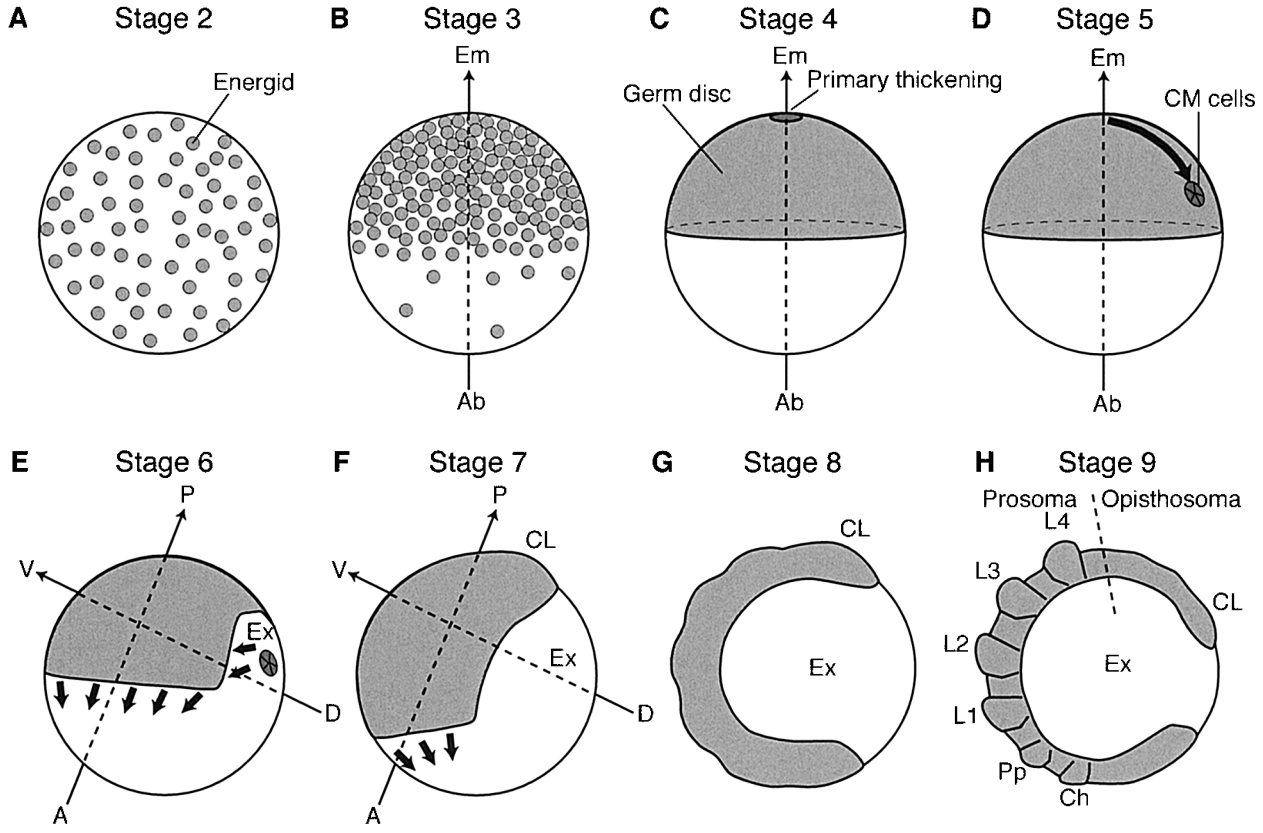

Fig. 1. The stages of *Achaearanea* embryogenesis. Stages 1 to 8 have been defined in the previous study (Akiyama-Oda and Oda, 2003). (A) Stage 2. The energids (shaded circles) appear at the periphery of the egg, and undergo synchronous cleavages. (B) Stage 3. The energids shift toward one pole of the egg along the surface. This pole is designated the embryonic (Em) pole, and the opposite pole the abembryonic (Ab) pole. (C) Stage 4. The energids settle and form a germ disc (shaded area). Cells are internalzied at the embryonic pole to form the primary thickening. (D) Stage 5. Some of the internalized cells, which are the cumulus mesenchymal (CM) cells, migrate in a cluster toward the rim of the germ disc (thick arrow). (E) Stage 6. Germ disc cells migrate in directions indicated by thick arrows, with the extraembryonic area (Ex) formed and expanded. During this stage, the radially symmetrical germ disc is converted into a fan-like shape with the AP and DV axes. (F) Stage 7. The fan-shaped embryo is transformed into a germ band with metameric morphologies. The previous central region of the germ disc develops into the caudal lobe (CL). (G) Stage 8. The germ band continues to extend (as indicated by thick arrows in F), and nascent limb buds appear. (H) Stage 9. The limb buds extend distally. L1 to L4 indicate the limb buds for the first to fourth walking legs, and Ch and Pp indicate those for the chelicera and pedipalp, respectively. The dotted line indicates the boundary between the prosoma and the opisthosoma.

These include cumulus mesenchymal (CM) cells, that are characterized by *At.dpp* expression, and some *At.fkh*-expressing cells (Akiyama-Oda and Oda, 2003). However, it is not known whether the *Achaearanea* mesoderm can be characterized molecularly in the same manner as the mesoderm in the *Drosophila* embryo. In this study, we cloned *A. tepidariorum* genes related to *Drosophila twi* and *sna*, designated *At.twi* and *At.sna,* respectively, to examine whether these genes can help to identify the mesoderm cells in developing embryos of the spider. Whole-mount in situ hybridization revealed that *At.twi*, but not *At.sna*, appears to be expressed in likely mesoderm cells. Thus, we propose that *At.twi* can be used as a molecular marker for analyzing the development of the spider mesoderm. Comparison of the expression patterns of *twi* and *At.twi* revealed divergent aspects of mesoderm development in the fly and spider.

MATERIALS AND METHODS

Animals

The spider *Achaearanea tepidariorum* was used in our experiments. Embryos were obtained as described previously (Akiyama-Oda and Oda, 2003). Stages 1 to 8 of embryonic development have been defined in the previous study (Fig. 1; Akiyama-Oda and Oda, 2003). Stage 9 is the period during which the nascent limb buds extend distally. Stage 10 is the period during which the extending limbs become segmented and the germ band splits to shift laterally.

cDNA cloning

To isolate *Achaearanea* homologs of the *Drosophila twi* and *sna* genes, we initially performed polymerase chain reactions (PCR) using degenerate primers. The following primers were used: *twi* forward primer, 5' tngcnaa(t/c)gtn(a/c)gnga(a/g)(a/c)g 3' (for the amino acid sequence (M/L)ANVRER); *twi* forward primer for nested PCR, 5' gtn(a/c)gnga(a/g)(a/c)gnca(a/g)(a/c)gnac 3' (for the amino acid sequence VRERQRT); *twi* reverse primer for the first and nested PCR, 5' a(a/g)(t/c)ttnt(a/g)ngt(t/c)tg(a/g/t)at(t/c)tt 3' (for the amino acid sequence LKLTQIK); *sna* forward primer, 5' aa(a/g)atgca(t/c)at(a/t/c)(a/c)gnacnca 3' (for the amino acid sequence KMHIRTH); *sna* reverse primer, 5' aangg(t/c)tt(t/c)tcnccngt(a/g)tg 3' (for the amino acid sequence FPKEGTH); *sna* forward primer for nested PCR, 5' gnacnca(t/c)acn(t/c)tnccntg 3' (for the amino acid sequence RTHTLPC); *sna* reverse primer for nested PCR, 5' gt(a/g)tgngtnc(g/t)(a/t/g)at(a/g)tgncc 3' (for the amino acid sequence THTRIHG). cDNA prepared from embryos and larvae were used as the template.

To isolate cDNA clones, digoxigenin (DIG)-labeled probes for the amplified fragments were prepared using a PCR DIG Probe Synthesis Kit (Roche). Two cDNA libraries of embryos and hatched prelarvae (Akiyama-Oda and Oda, 2003) were screened with the probes. Three clones for *At.twi* and one for *At.sna* were obtained. Both strands of the representative *At.twi* and *At.sna* clones were sequenced, revealing that these clones cover the entire or nearly entire coding regions of the mRNAs. However, the translation start site for *At.twi* mRNA was not determined with confidence since no in-frame stop codon was identified upstream of the first methionine in the isolated cDNA clones. In the *At.sna* clone, a potentially artifactual deletion of one nucleotide was detected. The DNA fragments covering the site were amplified by RT-PCR to determine the authentic sequence of *At.sna*. The *At.twi* and *At.sna* sequences are available from the DNA data bank of Japan (DDBJ) with the following Accession numbers: *At.twi*, AB167807; *At.sna*, AB167392.

Molecular phylogenetic analysis

The deduced amino acid sequences of the bHLH domains of *At.twi* and other *twi*-related genes as well as the zinc finger-containing regions of *At.sna* and other *sna*-related genes were aligned manually. Phylogenetic trees were constructed by the neighbor-joining method (Saitou and Nei, 1987) using PHYLIP (Felsenstein, 1993). Confidence in the phylogenies was assessed by bootstrap resampling of the data sets.

Whole-mount *in situ* hybridization

For whole-mount *in situ* hybridization, spider embryos were fixed as described previously (Akiyama-Oda and Oda, 2003). RNA probes were prepared using T7 RNA polymerase (Stratagene) and DIG RNA Labeling Mix (Roche). The first 916 bp of *At.twi* cDNA including the entire bHLH domain, and the 1692 bp region of *At.sna* cDNA (nt180-1871), which contains all the zinc finger motifs, were used as templates. Hybridization, washes and detection were performed as described previously (Akiyama-Oda and Oda, 2003). Some embryos were counterstained with the anti-pMAD antibody PS1(Persson *et al*., 1998).

Sectioning

Stained embryos were dehydrated in a graded ethanol-xylene series, embedded in TissuePrep (Fisher Scientific), and then serially sectioned at 5 μm thickness.

RESULTS AND DISCUSSION

Cloning of *A. tepidariorum* genes related to *twi* and *sna*

A. tepidariorum cDNAs related to *twi* and *sna* were cloned. The details of each cDNA sample are described below and in the Materials and Methods.

At.twi

The isolated cDNA clone encoded a polypeptide of 221 or more amino acids with a bHLH domain and a WR motif characteristic of Twist proteins (Fig. 2A). The bHLH domain displayed 61–69% amino acid identity with those in the Twist proteins of *Drosophila*, jellyfish, mollusk, leech, lancelet and mouse, compared to the 54%, 47% and 43% identity that it shared with the bHLH domain of the *Drosophila* non-Twist-class bHLH proteins Hand, Fer1 and Dimm, respectively. Based on the topology of a phylogenetic tree constructed using the bHLH domain sequences (Fig. 2C), the isolated gene was found to belong to the *twist* family. Accordingly, the gene was designated *At.twist (At.twi)*.

At.sna

Analysis of the isolated cDNA clone and amplified cDNA fragments revealed a polypeptide of 303 amino acids with five zinc finger motifs. The amino acid sequences of these motifs were highly similar to those found in *Drosophila* Sna, Escargot and Worniu and other animal Snail/Slug-class proteins (Fig. 2B). The isolated gene was classified into the *snail/slug* family, based on phylogenetic analyses using the sequences of the regions encompassing zinc finger II-V motifs (Fig. 2D). Accordingly, the gene was designated *At.snail* (*At.sna*). *At.sna* was most closely related to *Cs.sna*, a *snail* homolog in *Cupienius salei,* another spider species (Weller and Tautz, 2003).

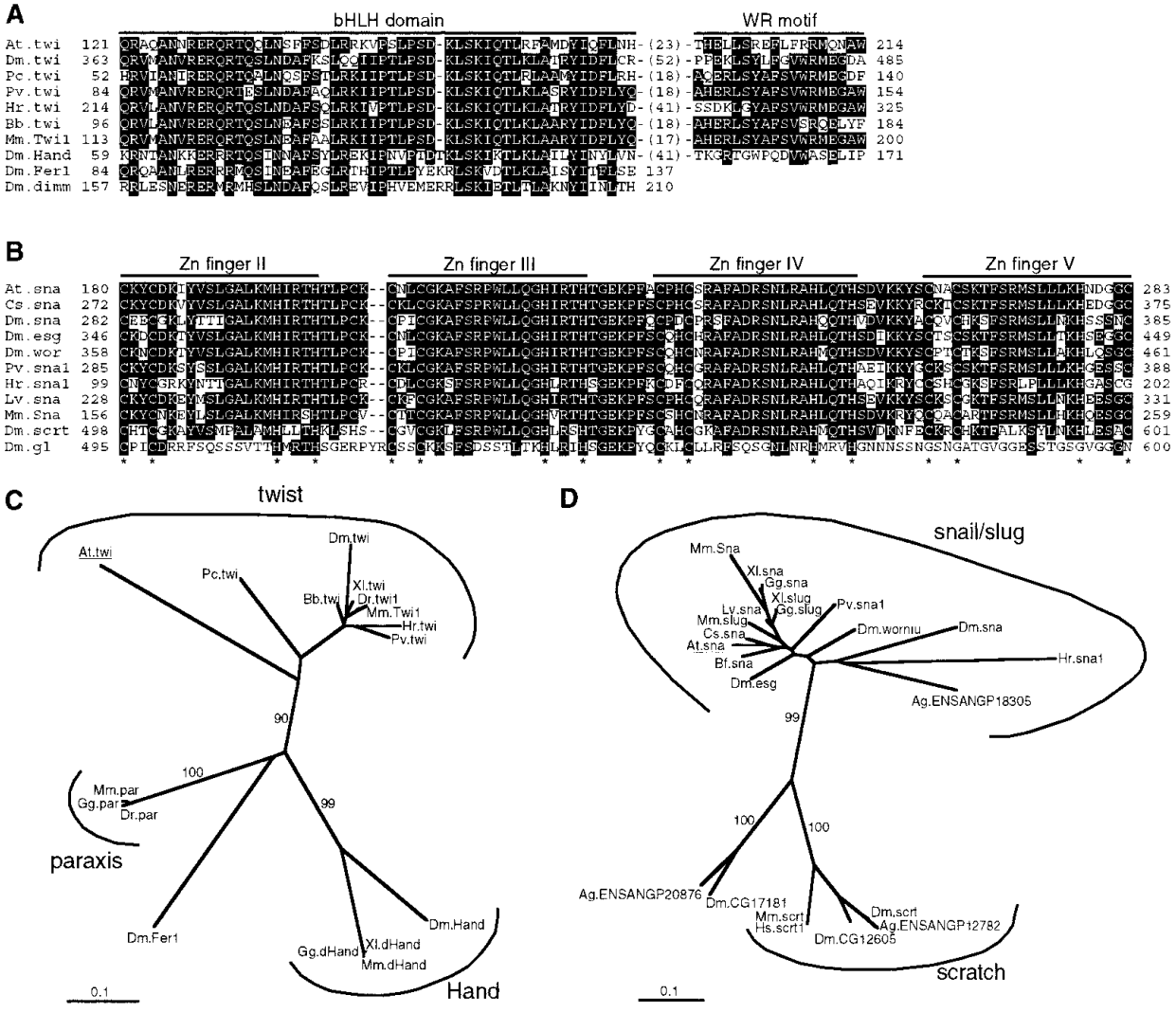

Fig. 2. (A, B) Alignment of the amino acid residues of the bHLH domains and the WR motifs of At.twi and other Twi-related proteins (A) and of the zinc finger II -V domains of At.sna and other Sna-related proteins (B). Identical residues are highlighted. Gaps were introduced to optimize the alignments (indicated by dashes). Numbers in parentheses represent the number of residues omitted at the indicated sites. Asterisks indicate the cysteine and histidine residues characteristic of zinc fingers. (C, D) Molecular phylogenetic trees constructed by the neighbor-joining method based on the alignment of the bHLH domain (C) and zinc finger II-V domains (D). The numbers at the internal branches are bootstrap values (%). Accession numbers of the proteins used are as follows: At.twi (AB167807), Dm.twi (S00995), Pc.twi (CAC12667), Pv.twi (AAL15167), Hr.twi (AAL05567), Bb.twi (O96642), Dm.Hand (NP_609370), Dm.Fer1 (NP_524251), Dm.dimm (NP_523611), At.sna (AB167392), Cs.sna (CAE00182), Dm.sna (NP_476732), Dm.esg (NP_476600), Dm.wor (AAF12733), Pv.sna1 (AAL06240), Hr.sna1 (AAL05564), Lv.sna (AAB67715), Dm.scrt (AAA91035), Dm.gl (P13360), Dr.par (NP_571047), Dr.twi1 (NP_571059), Gg.dHand (Q90690), Gg.par (AAC60208), Mm.dHand (AAC52338), Mm.par (Q60756), Mm.twi1 (NP_035788), Xl.twi (P13903), Xl.dHand (P57101), Ag.ENSANGP12782 (XP_308953), Ag.ENSANGP18305 (XP_317196), Ag.ENSANGP20876 (XP_315399), Bf.sna (AAC35351), Dm.CG12605 (NP_647845), Dm.CG17181 (NP_612040), Gg.slug (I50738), Gg.sna (CAA71033), Hs.scrt1 (NP_112599), Mm.scrt (NP_570963), Mm.slug (NP_035545), Mm.Sna (NP_035557), Xl.slug (Q91924), Xl.sna (P19382). Abbreviations of species are as follows: Ag, *Anopheles gambiae*; At, *Achaearanea tepidariorum*; Bb, *Branchiostoma belcheri*; Bf, *Branchiostoma floridae*; Cs, *Cupiennius salei*; Dm, *Drosophila melanogaster*; Dr, *Danio rerio*; Gg, *Gallus gallus*; Hr, *Helobdella robusta*; Hs, *Homo sapiens*; Lv, *Lytechinus variegates*; Mm, *Mus musculus*; Pc, *Podocoryne carnea*; Pv, *Patella vulgata*; Xl, *Xenopus laevis*.

At.twi transcripts are expressed in mesoderm cells

We examined the expression patterns of *At.twi* transcripts in spider embryos by whole-mount *in situ* hybridization. *At.twi* transcripts were not detected before late stage 5, when the CM cells reached the periphery of the germ disc (Akiyama-Oda and Oda, 2003). At early stage 6, *At.twi* transcripts were detected in cells located at the polar and equatorial areas of the embryo (Fig. 3A). In the initial pattern of *At.twi* expression, no reproducible asymmetry could be recognized with respect to the embryonic-abembryonic axis. As the extra-embryonic area expanded, more cells expressed *At.twi* transcripts (Fig. 3B). The *At.twi*-expressing cells became distributed nearly uniformly in the embryonic area. At these initial stages, some *At.twi*-expressing cells were found in the sur-

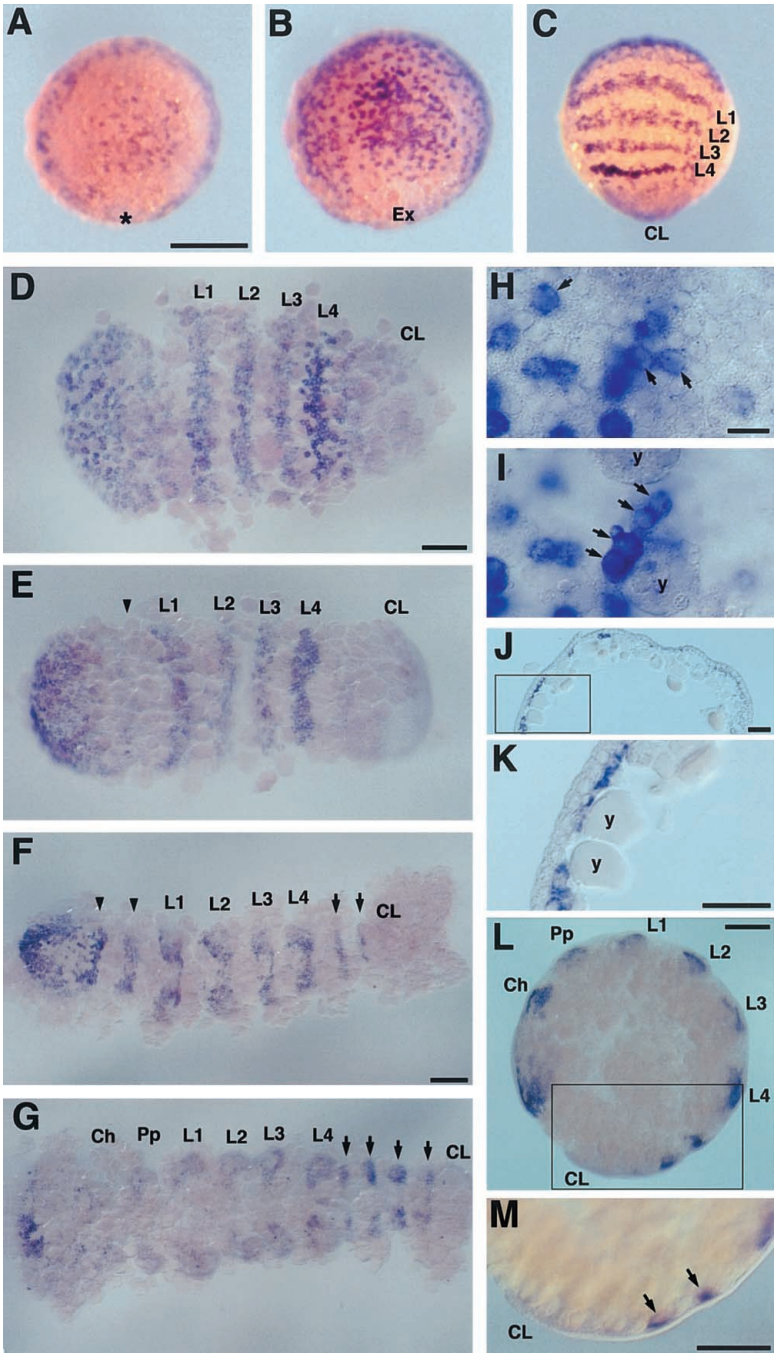

Fig. 3. Expression patterns of *At.twi* transcripts as revealed by whole-mount *in situ* hybridization. Signals of the *At.twi* transcripts are presented in purple. (A) An early stage 6 embryo viewed from the top of the germ disc. This embryo was also stained for pMAD (brown) to determine its orientation. The asterisk indicates the site of the germ disc rim at which the cumulus arrived. (B) A mid-stage 6 embryo viewed from the prospective caudal side. The emerging extra-embryonic area (Ex) shows little *At.twi* expression. (C) A stage 7 embryo viewed from the ventral side. Anterior is to the top. CL, caudal lobe; L1 to L4, first to fourth walking legs. (D–G) Flat preparations of embryos at stage 7 (D), stage 8 (E) and stage 9 (F, G). Anterior is to the left. One anterior domain and the following four stripes of *At.twi* expression are seen in the stage 7 embryo (D). The four stripes correspond to the segments bearing walking legs (L1–L4). The anterior domain was subdivided to give rise to two additional stripes (arrowheads) that correspond to the chelicerae (Ch) and pedipalps (Pp). In opisthosomal segments produced from the caudal lobe (CL), stripes or patches of *At.twi* expression are seen (arrows). (H, I) Close-up images showing the polar area of an embryo at early stage 6. The focus was adjusted to the surface epithelial layer for the first image (H), and shifted a little deeper into the interior of the embryo for the second image (I). Arrows indicate the *At.twi*-expressing cells in focus. y, yolk. (J, K) Longitudinal section of a stage 7 embryo. Anterior is to the left. The area boxed in J is magnified in K. *At.twi*-expressing cells are situated just beneath the surface ectoderm. (L, M) A stage 9 embryo viewed from the lateral side. The area boxed in L is magnified in M. Expression stripes that appeared in the opisthosomal region (arrows) are situated just beneath the surface ectoderm. Expression is not detectable at the caudal lobe (CL). Scale bar: 250 μm in A–C; 100 μm in D–G, L, M; 25 μm in H–K.

face epithelial layer but other *At.twi*-expressing cells were located a little deeper than at the surface (Fig. 3H, I).

The stage 7 embryo, which is transforming into a germ band, showed one anterior domain and four stripes of *At.twi* expression (Fig. 3C, D). Sectioning of stained stage 7 embryos revealed that all the *At.twi*-expressing cells were situated just beneath the ectoderm (Fig. 3J, K). The four stripes were persistently seen at later stages (Fig. 3D–F), and probably correspond to the segments bearing walking legs. The fourth stripe displayed higher levels of *At.twi* expression than the remaining three stripes (Fig. 3C–E). The anterior domain of *At.twi* expression was sequentially subdivided to produce two stripes (Fig. 3D–F). These two stripes probably correspond to the chelicerae and pedipalps. Each of the six, in total, *At.twi* expression stripes at the prosomal region was laterally split into two large patches. These changes in the shapes of the *At.twi* expression domains occurred in accordance with the formation of the limb buds (Fig. 3E, F), although the expression gradually declined during limb bud extension (Fig. 3G). In embryos whose limb buds were extending, relatively high levels of *At.twi* expression remained detectable at the anterior terminal region (Fig. 3G).

At the formed caudal lobe, little *At.twi* expression was observed (Fig. 3C–E). However, in the segments produced from the caudal lobe, expression stripes appeared (Fig. 3F, G, arrows). Like the prosomal stripes, these opisthosomal stripes were also situated just beneath the ectoderm (Fig. 3L, M). At later stages, each was laterally split into two patches (Fig. 3G).

We speculated that the cells expressing *At.twi* are mesoderm cells for four reasons, as follows. First, at least in stage 7 and older embryos, all the *At.twi*-expressing cells were situated just beneath the surface ectoderm. Second, the *At.twi*-expressing cells, unlike typical endoderm cells, became metamerically arranged. Third, in stage 9 embryos, most of the *At.twi*-expressing cells present in the prosomal segments were associated with the forming limb buds, where somatic and visceral mesoderm cells have been observed morphologically (Montgomery, 1909). Fourth, in *Achaearanea*, the central nervous system develops from the surface ectoderm at stage 9 and later in a way similar to that described in *Cupienius* (Stollewerk *et al.*, 2001; Y. A. and H. O., unpublished observations). It is likely that the *At.twi*-expressing cells are distinct from the internalized neural cells. The distributions of the *At.twi*-expressing cells pre-

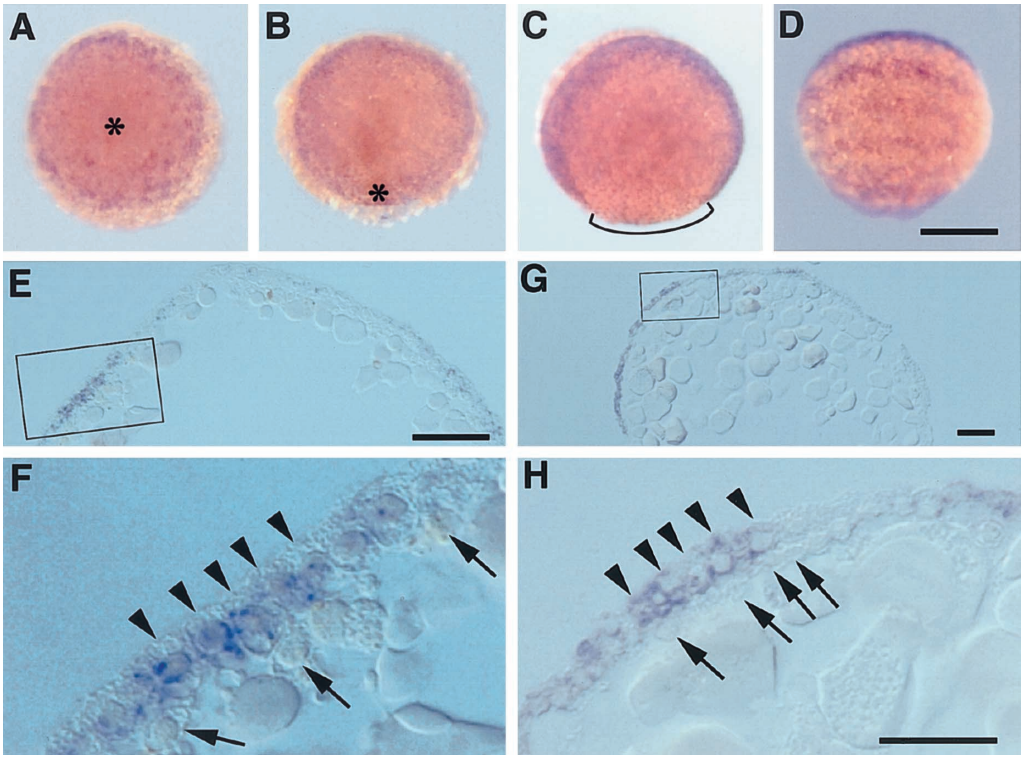

Fig. 4. Expression patterns of *At.sna* transcripts as revealed by whole-mount *in situ* hybridization. Signals of the *At.sna* transcripts are presented in purple. Embryos shown in A–C and E were also stained for pMAD (brown). (A) An early stage 5 embryo viewed from the top of the germ disc. The asterisk indicates the center of the germ disc. (B) An early stage 6 embryo viewed from the top of the germ disc. *At.sna* expression is detected in a broad ring of the germ disc area. Around the polar area, lower levels of *At.sna* expression are observed. The asterisk indicates the site of the germ disc rim at which the cumulus arrived. (C) A mid-stage 6 embryo viewed from the prospective caudal side. The bracket indicates the extra-embryonic area, which displays little or no *At.sna* expression. (D) A stage 7 embryo viewed from the ventral side. Anterior is to the top. Metameric patterns of expression are observed. (E, F) Longitudinal section of a stage 5 embryo. The area boxed in E is magnified in F. (G, H) Longitudinal section of a stage 7 embryo. Anterior is to the left. The area boxed in G is magnified in H. *At.sna* expression is detectable in surface cells (arrowheads) but not in internal cells (arrows). Scale bar: 250 μm in A–D; 50 μm in E, G; 25 μm in F, H.

sented here are similar to those of cells that Montgomery has described as mesentoblasts and mesoblasts (Montgomery, 1909). We propose that *At.twi* can be used as a marker for analyzing mesoderm development in the spider. Moreover, our observations suggest that *twi* and *At.twi* play conserved roles in the mesoderm development of the fly and spider.

At.sna transcripts are expressed in part of the ectoderm

The expression patterns of *At.sna* transcripts were also examined by whole-mount *in situ* hybridization. *At.sna* transcripts were detected in a broad ring near the margin of the germ disc from late stage 4 or early stage 5, and similar patterns persisted up to the beginning of stage 6 (Fig. 4A–C). Sectioning of stained stage 5 embryos revealed that the *At.sna*-expressing cells were located only in the surface cell layer (Fig. 4E, F). As the extra-embryonic area expanded, this area displayed lower levels of expression compared to the embryonic area (Fig. 4C). At stage 7, *At.sna* expression was seen in stripes (Fig. 4D). Although this expression pattern was, at a glance, similar to that of *At.twi* at the corresponding stage, the *At.sna* expression stripes were located in the surface ectoderm with no expression in the inner layer (Fig. 4G, H). At later stages of embryogenesis, *At.sna* transcripts were detected in the central nervous system (data not shown), consistent with the expression pattern of *Cs.sna* (Stollewerk *et al*., 2001; Weller and Tautz, 2003). These observations indicate that *At.sna* is expressed in part of the ectoderm, but not in the *twi*-expressing mesoderm. Our data do not suggest that the role for *snail* in the mesoderm formation of the fly is conserved in the spider.

Divergent aspects of mesoderm development in the fly and spider

Comparison of the expression patterns of *twi* and *At.twi*

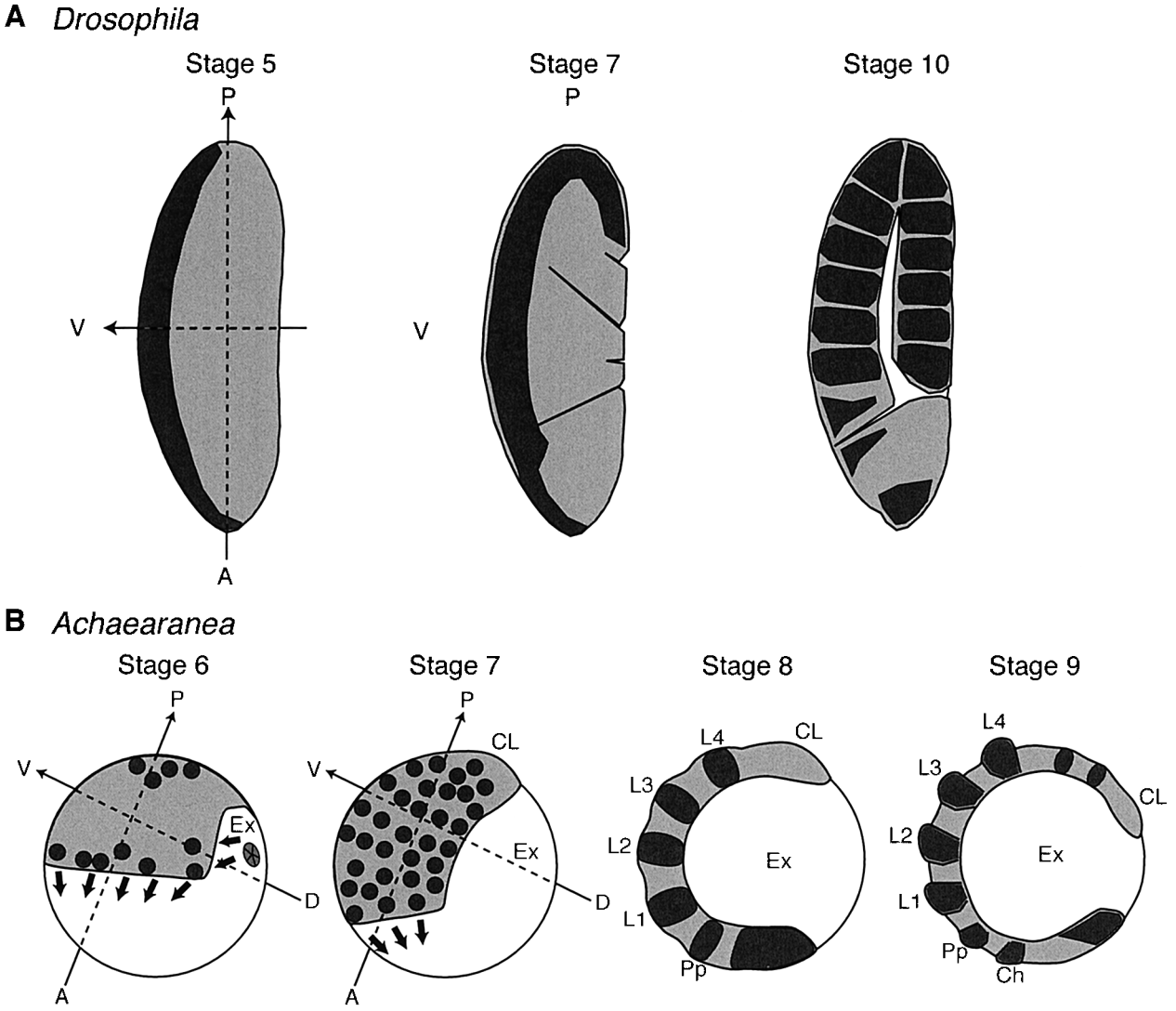

Fig. 5. Comparison of *twi* expression between *Drosophila* and *Achaearanea*. (A) Schematic illustrations showing *twi* expression patterns in the stage 5, 7 and 10 embryos of *Drosophila* (based on Bate, 1993). (B) Schematic illustrations showing *At.twi* expression patterns in the stage 6, 7, 8 and 9 embryos of *Achaearanea*. The embryonic area of each embryo is lightly shaded, and the cells (indicated by circles) or domains expressing *twi* or *At.twi* are darkly shaded. See the legend of Fig. 1 for abbreviations.

revealed divergent aspects of mesoderm development in *Drosophila* and *Achaearanea* (Fig. 5). In the fly embryo, all the mesoderm arises from the future ventral side (Fig. 5A). In contrast, in the spider embryo, the initial distribution of *At.twi* transcripts was not ventrally localized; instead, this distribution was rather symmetric with respect to the embryonic-abembryonic axis (Fig. 3A). The emerging asymmetry of *At.twi* expression during stage 6 (Figs 3B, 5B) appeared to be associated with the formation of the extra-embryonic area. The *At.twi* expression pattern within the embryonic area showed little unevenness along the emerging DV axis until the limb buds began to form. These observations indicate that the relationship between DV pattern formation and mesoderm formation differs in the fly and spider. In the *Drosophila* embryo, all prospective mesoderm cells are internalized from the ventral side within a short period, and this process can be observed (Sweeton *et al*., 1991; Kam *et al*., 1991; Oda and Tsukita, 2001). In the spider embryo, however, it was not so easy to determine from where and how the mesoderm was internalized. This difficulty may be at least partially due to asynchronous internalization of prospective mesoderm cells, as *At.twi*-expressing cells were found both at the surface and inner layers in the same germ discs (Fig. 3H, I). However, we could not reconstruct the dynamic processes of cell behavior and gene expression with any certainty. Nonetheless, the initial patterns of *At.twi* expression (Figs 3A, 5B) may suggest that the central and peripheral areas of the germ disc are the sites of mesoderm internalization in the *Achaearanea* embryo. Invagination of the individual cells that have stochastically started to express *At.twi* at the surface might explain the mesoderm internalization. The mechanism by which the *At.twi* expression is initiated is an interesting issue to be studied in the future, which will clarify the difference between the fly and spider.

In the *Drosophila* embryo, *twi* transcription is initiated simultaneously in all prospective mesoderm cells, and mesoderm differentiation proceeds synchronously in all segments. Apparently, this is not the case in the *Achaearanea* embryo. The number of *At.twi*-expressing cells increased progressively during early and mid stage 6 (Fig. 3A, B). This increase may be due to initiation of *At.twi* transcription as well as to cell division. The four expression stripes of *At.twi* corresponding to the segments bearing walking legs emerged during the formation of the germ band, when *At.sna* and many other genes showed striped expression in the surface ectoderm (Fig. 4D; our unpublished data). Thus, it appears that the patterning of the prosomal mesoderm is accompanied with that of the surface ectoderm. The appearance of new *At.twi* expression stripes at the growing opisthosomal region during stages 8 and 9 (Fig. 5B) is the result of initiation of *At.twi* transcription rather than subdivision of cell populations with persistent *At.twi* expression, since we have not observed intermediate states of such subdivision. Interestingly, in contrast to the opisthosomal region, the *At.twi* expression stripes corresponding to the chelicerae and pedipalps appeared to be formed as a result of sequential subdivision (Fig. 3D–F). In the prosomal and opisthosomal regions, different mechanisms may regulate the initiation of *At.twi* transcription. What cellular and molecular mechanisms cause the segmentation of the mesoderm in the spider embryo remain to be elucidated.

We suggest that there are crucial differences in the way the mesoderm develops in the fly and spider. Investigation of the cellular and molecular mechanisms underlying these differences will contribute to a better understanding of the ancestral mode of mesoderm development in the phylum Arthropoda. Although possible variations in the mode of mesoderm development among spiders as well as chelicerates will be considered, we believe the *twist* family genes will be useful in comparative analyses that aim to reconstruct the evolution of the arthropod mesoderm.

ACKNOWLEDGMENTS

We thank Dr. Tetsuya Tabata for the PS1 antibody, Ms. Masami Irie for technical assistance, and Dr. Ryuichiro Machida and all the members of JT Biohistory Research Hall for discussions and encouragement.

REFERENCES

Akiyama-Oda Y, Oda H (2003) Early patterning of the spider embryo: a cluster of mesenchymal cells at the cumulus produces Dpp signals received by germ disc epithelial cells. Development 130: 1735–1747

Alberga A, Boulay JL, Kempe E, Dennefeld C, Haenlin M (1991) The *snail* gene required for mesoderm formation in *Drosophila* is expressed dynamically in derivatives of all three germ layers. Development 111: 983–993

Anderson DT (1973) Embryology and phylogeny in annelids and arthropods. In “International series of monographs in pure and applied biology. Division Zoology, Vol 50” Ed by GA Kerkut, Pergamon Press, Oxford

Bate M (1993) The mesoderm and its derivatives. In “The Development of *Drosophila melanogaster*.” Ed by M Bate and A Martinez Arias, Cold Spring Harbor Laboratory Press, New York, pp 1013–1090

Boore JL, Lavrov DV, Brown WM (1998) Gene translocation links insects and crustaceans. Nature 392: 667–668

Boulay JL, Dennefeld C, Alberga A (1987) The *Drosophila* developmental gene snail encodes a protein with nucleic acid binding fingers. Nature 330: 395–398

Chasan R, Anderson KV (1993) Maternal control of dorsal-ventral polarity and pattern in the embryo. In “The Development of *Drosophila melanogaster*.” Ed by M Bate and A Martinez Arias, Cold Spring Harbor Laboratory Press, New York, pp 387–424

Chen G, Handel K, Roth S (2000) The maternal NF-kB/Dorsal gradient of *Tribolium castaneum*: dynamics of early dorsoventral patterning in a short-germ beetle. Development 127: 5145–5156

Cook CE, Smith ML, Telford MJ, Bastianello A, Akam M (2001) Hox genes and the phylogeny of the arthropods. Curr Biol 11: 759–763

Felsenstein J (1993) PHYLIP (Phylogeny Inference Package). Department of Genetics, University of Washington, Seattle

Friedrich M, Tautz D (1995) Ribosomal DNA phylogeny of the major extant arthropod classes and the evolution of myriapods. Nature 376: 165–167

Furlong EEM, Andersen EC, Null B, White KP, Scott MP (2001) Patterns of gene expression during *Drosophila* mesoderm development. Science 293: 1629–1633

Giribet G, Edgecombe GD, Wheeler WC (2001) Arthropod phylogeny based on eight molecular loci and morphology. Nature 413: 157–161

Harfe BD, Gomes AV, Kenyon C, Liu J, Krause M, Fire A (1998) Analysis of a *Caenorhabditis elegans* Twist homolog identifies conserved and divergent aspects of mesodermal patterning. Genes Dev 12: 2623–2635

Holm Å (1940) Studien über die Entwicklung und Entwicklungsbiologie der Spinnen. Zool Bidr Uppsala 19: 1–214

Holm Å (1952) Experimentelle Untersuchungen über die Entwicklung und Entwicklungsphysiologie des Spinnenembryos. Zool Bidr Uppsala 29: 293–424

Hopwood ND, Pluck A, Gurdon JB (1989) A Xenopus mRNA related to Drosophila twist is expressed in response to induction in the mesoderm and the neural crest. Cell 59: 893–903

Imai KS, Satoh N, Satou Y (2003) A Twist-like bHLH gene is a downstream factor of an endogenous FGF and determines mesenchymal fate in the ascidian embryos. Development 130: 4461–4472

Kam Z, Minden JS, Agard DA, Sedat JW, Leptin M (1991) *Drosophila* gastrulation: analysis of cell shape changes in living embryos by three-dimensional fluorescence microscopy. Development 112: 365–370

Lee HH, Frasch M (2000) Wingless effects mesoderm patterning and ectoderm segmentation events via induction of its downstream target sloppy paired. Development 127: 5497–5508

Leptin M (1991) *twist* and *snail* as positive and negative regulators during *Drosophila* mesoderm development. Genes Dev 5: 1568–1576

Leptin M, Grunewald B (1990) Cell shape changes during gastrulation in *Drosophila*. Development 110: 73–84

Martindale MQ, Pang K, Finnerty JR (2004) Investigating the origins of triploblasty: 'mesodermal' gene expression in a diploblastic animal, the sea anemone *Nematostella vectensis* (phylum, Cnidaria; class, Anthozoa). Development 131: 2463–2474

Montgomery TH Jr (1909) The development of Theridium, an Aranead, up to the stage of reversion. J Morph 20: 297–352

Nederbragt AJ, Lespinet O, van Wageningen S, van Loon AE, Adoutte A, Dictus WJAG (2002) A lophotrochozoan *twist* gene is expressed in the ectomesoderm of the gastropod mollusk *Patella vulata*. Evol Dev 4: 334–343

Oda H, Tsukita S (2001) Real-time imaging of cell-cell adherens junctions reveals that *Drosophila* mesoderm invagination begins with two phases of apical constriction of cells. J Cell Sci 114: 493–501

Persson U, Izumi H, Souchelnytskyi S, Itoh S, Grimsby S, Engström U, Heldin C-H, Funa K, ten Dijke P (1998) The L45 loop in type I receptors for TGF-b family members is a critical determinant in specifying Smad isoform activation. FEBS Lett 434: 83–87

Riechmann V, Irion U, Wilson R, Grosskortenhaus R, Leptin M (1997) Control of cell fates and segmentation in the *Drosophila* mesoderm. Development 124: 2915–2922

Saitou N, Nei M (1987) The neighbour-joining method: A new method for reconstructiong phylogenetic trees. Mol Biol Evol 4: 406–425

Seitz KA (1966) Normale Entwicklung des Arachniden-Embryos *Cupiennius salei* Keyserling und seine Regulationsbefähigung nach Röntgenbestrahlungen. Zool Jb Anat Bd 83: 327–447

Simpson P (1983) Maternal-zygotic gene interactions during formation of the dorsoventral pattern in *Drosophila* embryos. Genetics 105: 615–632

Sommer RJ, Tautz D (1994) Expression patterns of *twist* and *snail* in *Tribolium* (Coleoptera) suggest a homologous formation of mesoderm in long and short germ band insects. Dev Genet 15: 32–37

Spring J, Yanze N, Middel AM, Stierwald M, Gröger H, Schmid V (2000) The mesoderm specification factor Twist in the life cycle of jellyfish. Dev Biol 228: 363–375

St Johnston D, Nüsslein-Volhard C (1992) The origin of pattern and polarity in the *Drosophila* embryo. Cell 68: 201–219

Staehling-Hampton K, Hoffmann FM, Baylies MK, Rushton E,Bate M (1994) dpp induces mesodermal gene expression in *Drosophila*. Nature 372: 783–786

Stollewerk A, Weller M, Tautz D (2001) Neurogenesis in the spider *Cupiennius salei*. Development 128: 2673–2688

Suzuki H, Kondo A (1995) Early embryonic development, including germ-disk stage, in the Theridiid spider *Achaearanea japonica* (Bös. et Str.). J Morphol 224: 147–157

Sweeton D, Parks S, Costa M, Wieschaus E (1991) Gastrulation in *Drosophila*: The formation of the ventral furrow and posterior midgut invaginations. Development 112: 775–789

Tapanes-Castillo A, Baylies MK (2004) *Notch* signaling patterns *Drosophila* mesodermal segments by regulating the bHLH transcription factor *twist*. Development 131: 2359–2372

Thisse B, Stoetzel C, Gorostiza-Thisse C, Perrin-Schmitt F (1988) Sequence of the *twist* gene and nuclear localization of its protein in endomesodermal cells of early *Drosophila* embryos. EMBO J 7: 2175–2183

Thisse C, Thisse B (1992) Dorsoventral development of the *Drosophila* embryo is controlled by a cascade of transcriptional regulators. Development Supplement: 173–181

Weller M, Tautz D (2003) Prospero and Snail expression during spider neurogenesis. Dev Genes Evol 213: 554–566

Yasui K, Zhang S, Uemura M, Aizawa S, Ueki T (1998) Expression of a *twist*-related gene, *Bbtwist*, during the development of a lancelet species and its relation to cephalochordate anterior structures. Dev Biol 195: 49–59

Yoshikura M (1975) Comparative embryology and phylogeny of arachnida. Kumamoto J Sci Biol 12: 71–142

(Received November 8, 2004 / Accepted November 24, 2004)